A sensitive and versatile torque magnetometer for use in high magnetic fields

S. A. J. Wiegers[a)]
Grenoble High Magnetic Field Laboratory, Max-Planck Institute für Festkörperforschung-Centre National de la Recherche Scientifique, BP 166, F-38042 Grenoble Cedex 9, France and Nijmegen High Field Magnet Laboratory and Research Institute for Materials, University of Nijmegen, Nijmegen, The Netherlands

A. S. van Steenbergen and M. E. Jeuken
Nijmegen High Field Magnet Laboratory and Research Institute for Materials, University of Nijmegen, Nijmegen, The Netherlands

M. Bravin, P. E. Wolf, and G. Remenyi
CRTBT-CNRS, BP 166, F-38042 Grenoble, France

J. A. A. J. Perenboom and J. C. Maan
Nijmegen High Field Magnet Laboratory and Research Institute for Materials, University of Nijmegen, Nijmegen, The Netherlands

(Received 17 February 1998; accepted for publication 1 April 1998)

We describe the design and construction of a sensitive dc torque magnetometer suitable for liquid as well as solid state samples. It can be used from room temperature down to very low temperatures (mK range) in magnetic fields produced either by superconducting or resistive magnets, in particular in the high fields ($B \approx 30$ T) produced by Bitter and hybrid magnets. The highest resolution that we have attained so far is about 0.3 pNm, which is mainly the result of a symmetric design. In typical laboratory conditions (at $B = 10$ T) this corresponds to a magnetization resolution of about 3×10^{-11} emu. Other features include modularity, linearity, feedback and forward bias capabilities, and an *in situ* calibration of the signal. © *1998 American Institute of Physics.* [S0034-6748(98)05106-5]

I. INTRODUCTION

In order to measure small magnetic moments in high magnetic fields (up to 30 T or more), one needs a sensitive magnetometer whose proper functioning is neither affected by the magnitude nor by spatial inhomogeneities or temporal fluctuations of the magnetic field. A mechanical torque magnetometer complies with these requirements and several designs have appeared in literature in recent years.[1–6] In these devices one generally uses a soft spring to convert a torque Γ into the displacement of a moving part with respect to a fixed body, which is capacitively detected. Thus the detected quantity is actually not the torque, but the displacement resulting from it. The magnitude of the spring constant K plays a role in the sensitivity $dC/d\Gamma$, where C represents the measured capacitance: the softer the spring is, the higher the sensitivity will be.

The resolution of torque magnetometers operating in high magnetic field is in many cases limited by mechanical noise δC_m rather than by electronic noise δC_e. Mechanical noise is induced by the coupling of vibrations of the fixed body of the device to the relevant motion of its moving part. These vibrations can, e.g., be caused by the violent acoustic environment presented by Bitter magnets, which are also part of so-called hybrid magnets in which the highest dc magnetic fields can be generated. In some instances these acoustic vibrations are strong enough to be noticed by the experimenter by putting one's hand on the cryostat. Under such circumstances, the resolution is not improved by reducing K.

The purpose of this article is to present a new type of torque magnetometer, which is inherently insensitive to mechanical noise. This insensitivity is obtained by the decoupling of transversal vibrations of the whole device from the relevant motion of the moving part of the magnetometer, using a very symmetric design of the moving part. This design is not only useful for measurements in resistive magnets, but is also well suited for high precision measurements in superconducting magnets.

The torque magnetometer (see Fig. 1) consists of a rotatable epoxy wheel (the rotor) suspended by a thin metal torsion wire inside a cylindrical housing (the stator). An important feature of this construction is that the center of mass of the rotor is nominally on the rotation axis (the torsion wire) and therefore only a very small coupling exists between a translation of the whole device and rotation of the wheel. A further advantage of this geometry is the cancellation of the isotropic background magnetization of the rotor. These features allow to accurately measure magnetization in both superconducting and in Bitter magnets. The observed increase of the mechanical noise level is less than a factor of 10 in a Bitter magnet compared to a superconducting magnet. Given the linear increase in sensitivity of the magnetometer with magnetic field, this implies a decrease in resolu-

[a)]Electronic mail: wiegers@sci.kun.nl

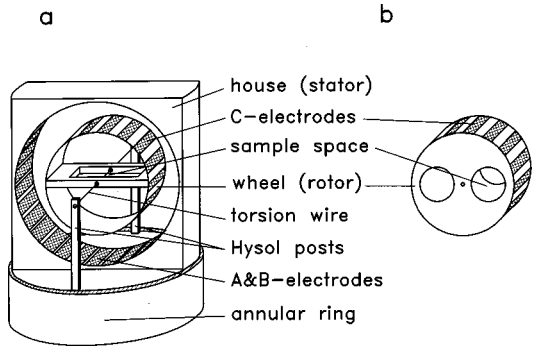

FIG. 1. Schematic drawing of the epoxy torque magnetometer showing also the different wheel design for solid state (a) and liquid samples (b). The size of the gap between the electrodes is exaggerated to show more clearly the electrode configuration.

tion of at most a mere factor of 5 in going from a superconducting to a Bitter magnet at their respective maximum magnetic field values.

Besides its high resolution, our design has a number of advantages compared to, e.g., (commercially available) cantilever based torque magnetometers.[7] First, our magnetometer is suitable for bulk solid state samples, metallic as well as insulating. One of the more prominent applications of our device, demonstrating its high resolution, is the measurement of the anisotropic magnetization of small samples mounted on relatively large substrates, like the de Haas van Alphen (dHvA) magnetization of a two-dimensional electron gas (2DEG).[8] Cantilever magnetometers cannot carry samples heavier than typically 10 mg due to the (unbalanced) gravitational force. For our solid state sample magnetometer this number is at least one order of magnitude higher, the weight of the rotor alone being about 200 mg.

Second, our design includes a version for liquid samples. An example with a liquid sample is provided by the measurement of the isotropic nuclear magnetization of liquid ^{3}He in high magnetic fields.[9]

In the following we will first present the working principle of the magnetometer and the construction details. Then we will discuss the performance and demonstrate its sensitivity by showing some results of measurements on a 2DEG and on liquid ^{3}He.

II. PRINCIPLE

In our epoxy magnetometer the torque exerted on the wheel is converted into a rotation, which is capacitively detected through a change in the overlapping surface area between the set of electrodes on the perimeter of the rotor and those on the inside of the stator (Fig. 1). The choice for epoxy as fabrication material is motivated by several requirements: weakly diamagnetic, nonmetallic, low mass, and easily machinable.

The magnetometer is sensitive to the torque $\boldsymbol{\Gamma}$, exerted by an anisotropic magnetic moment in a nonparallel magnetic field, $\boldsymbol{\Gamma}=\mathbf{M}\times\mathbf{B}$, or by an isotropic magnetic moment in a magnetic field gradient, $\boldsymbol{\Gamma}=\mathbf{r}\times(\mathbf{M}\cdot\boldsymbol{\nabla})\mathbf{B}$, where r represents the distance between the sample and the rotation axis.

In the general case both kinds of torque, anisotropic and isotropic, contribute to the measured torque, and one should be aware of this when the sample is not perfectly placed on the rotation axis and there is a field gradient present. This is the case when the sample is not located at the center of the magnet coil. On the other hand, this property can be used to distinguish between the different contributions to the magnetization, as has been elegantly shown, e.g., in the case of the mixed valence system HgSe:Fe.[10]

There are two designs for the rotor depending on whether the sample is a solid or a liquid. In the case of a solid state sample the rotor is a hollow cylinder with the sample platform symmetrically dividing the wheel into two parts. There are two mounting possibilities depending on the magnetic nature of the sample. If it has an anisotropic magnetization it is preferably mounted symmetrically in the center of the rotor in the rectangular space of the platform which is inclined with respect to the magnetic field. The inclination is usually about 30°, which is a compromise between sensitivity and not losing too much field parallel to the easy axis of the sample. A solid state sample having an isotropic magnetization has to be mounted close to the perimeter of the rotor for maximum sensitivity. In order to keep a symmetrical arrangement, it is necessary to mount a nonmagnetic dummy sample on the other side of the platform having approximately the same mass as the real sample so as to keep the center of mass on the rotation axis. Note that the former configuration is more sensitive than the latter, since for a typical Bitter magnet the value of B is about one order of magnitude larger than the maximum attainable value of $\nabla B \times r$.

Liquids have in general an isotropic magnetization which can only be measured in a magnetic field gradient. In this case, the wheel consists of a solid cylinder having two holes on either side of the rotation axis.[5,9] One hole is open to the outside, the other is closed with two caps. The two holes are of equal volume and are symmetrically positioned. The magnetometer is immersed in the liquid which will enter the open hole and will exert a force $M\nabla B$ on the walls of the hole. Note that it is not required that the hole be closed after the liquid has entered: one can simply regard the action of the magnetic force in the same way as the gravitational effect of immersing an object in a liquid (buoyancy). In this picture the gravitational field g is replaced by ∇B and the mass m by the magnetization M. This also makes clear that even liquid outside the hole may contribute to the signal if the center of mass is not on the torsion wire. Although a single open hole, or even just an asymmetric positioning of the torsion wire with respect to the center of mass of the wheel, would thus equally well produce a device sensitive to this magnetic gravitation effect, the asymmetry obviously does not fit our requirements of mechanical decoupling and low background presented above. Moreover, liquid located in an asymmetric part of the wheel may contribute to the magnetization signal in an uncontrollable fashion. Therefore, we have not tried to remove material from the wheel (to decrease its mass), but have kept the inherent symmetry of the cylinder intact. In view of the response time (see Sec. IV), this limits somewhat the smallest diameter that can be used for the torsion wire.

For both liquid and solid samples, the absolute magnetization can be determined provided the sensitivity of the device to the applied torque is known as well as the angle of the field with respect to the magnetic easy axis (resp. the field gradient) for a solid (resp. liquid) sample. Both the sensitivity of the device and the magnetic field profile can be conveniently measured by using a calibration coil mounted on the wheel, and by translating the whole device along the field axis.

III. DESIGN AND CONSTRUCTION

A. Wheel (rotor)

We will first discuss the magnetometer which is used for solid state samples. It consists of a thin hollow epoxy cylinder (the wheel or rotor), suspended by a thin metal wire in the center of an Araldite housing, as shown in Fig. 1(a). The wheel is about 0.25 mm in thickness, 6 mm wide, and has a 17.6 mm outer diameter. It is machined on a lathe from Hysol[11] and it has eight equally spaced 10^3-Å-thick Au electrodes (the C electrodes) evaporated on the outside. We have also used Ag painted electrodes but found it less accurate and more cumbersome to apply than the Au evaporation process. For this purpose an aluminum mask was made in which the wheel was held during evaporation. To obtain an homogeneous Au layer the wheel was rotating during the evaporation. For better adhesion a 100 Å Ti layer was first evaporated on the surface.

The wheel is divided into two halves by a 1.0-mm-thick Hysol platform of 6.0 mm width, which snugly fits in the center of the wheel and is glued to the wheel on both sides with Stycast 1266.[12] The platform is positioned with the aid of two identical solid half disks that are made to exactly fit inside the space in the wheel left by the platform. The platform has an open 4×6 mm^2 rectangular space in the middle where a solid state sample can be mounted, either on a thin piece of cigarette paper glued to the bottom of the platform, or just resting on the torsion wire and mechanically fixed to the platform with a little silicon grease. This ensures that the sample is as close as possible to the rotation axis. During sample mounting the wheel is prevented from rotating by inserting a thin piece of paper between the wheel and the housing. This avoids premature wire breakage. The sample is held just above the rectangular sample space with a pair of tweezers and then gently dropped. The sample can be safely lifted off the platform by sliding it first to a side using two tooth picks and then taking it off with a pair of tweezers. It takes about 15 min to half an hour to change sample, including cleaning the platform of excess grease.

In the case of a liquid sample, a solid wheel of similar outer dimensions is constructed, having a hole of a few mm diameter on either side of the rotation axis [see Fig. 1(b)]. One of these holes is open to the liquid, and the other one is closed with two caps in a ^{4}He gas atmosphere to avoid magnetic pollution by O_2.

The assembly consisting of the wheel plus platform plus the half disks are put in a lathe to drill two holes of 0.1 mm diameter and 1 mm length in the center of the platform, through which the torsion wire runs. In the case of the solid wheel, a ϕ 0.4 mm hole is drilled in which a ϕ 0.1–0.4 mm CuNi capillary is inserted. The distance by which the center of mass is off axis, can be determined by rotating the whole device by 90° and 180° around the torsion axis and measuring the angular deviation of the wheel between these and the normal position. The off-axis distance is usually found to be on the order of a few tens of microns (with noticeable exceptions down to 5 μm).

The torsion wire is a nonmagnetic phosphor–bronze wire or a manganin wire of about 5 mm length on each side of the wheel. The diameter of the wire ranges in practice between 25 and 100 μm. The lower limit is determined mainly by handling and break properties and by the requirement that the resonance frequency of the device is not too low (see Sec. IV). The upper limit is chosen such that the mechanical noise still dominates the electronic noise.

The electrical contract to the C electrodes is made by silver painting a thin strip on the side of the platform from the outermost of the wheel to the torsion wire in the center. The torsion wire is used to electrically connect the silver painted strip to a contact located on the bottom of the housing. In principle one could use for this purpose an additional phosphor–bronze wire attached to the platform, which offers the possibility to increase the spring constant or rotate the wheel to obtain a different orientation of the platform with respect to the field. A small coil (Cu wire, ϕ 15 μm) is mounted in the middle of the platform or around the wheel. It provides a known magnetic moment for calibration purposes, forward biasing, and feedback measurements. The leads are twisted and carefully guided along the rotation axis to avoid uncontrolled and hysteretic contributions of the soft Cu lead wires to the spring constant.

B. Housing

Being less fragile than the wheel, the housing is made of Araldite and has a hole of 18.0 mm inner diameter and 6 mm width to accommodate the rotor. On the inside of the hole, two sets each of eight Au electrodes are evaporated (the A and B electrodes) essentially in the same way as for the wheel electrodes. There is a gap of about 0.2 mm between the inner and outer electrodes of the device. The wire, by which the wheel is suspended, is stretched between two rectangular Hysol posts. These posts fit in a slot milled in the base of the housing and are mechanically fixed by an annular, tight fitting ring. The posts are bent inwards (about 0.3 mm at the top) to slightly overcompensate the difference in thermal contraction between the metallic torsion wire and the plastic parts when the device is at low temperature. In this way the wire always remains stretched.

To mount the wheel in the housing and to bend the posts, an auxiliary mounting device is used, which is schematically shown in Fig. 2. It consists of a brass holder, in which the bottom of the housing can be fixed, with two brass posts on either side (at the same lateral position as the Hysol posts) having small holes at the height of the torsion wire to guide and fix the torsion wire in. After the wheel has been centered in the housing and the Hysol posts have been bent inwards by two small screws in the brass posts of the mounting de-

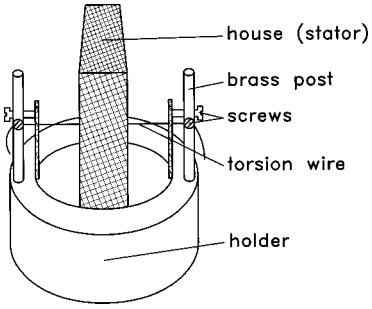

FIG. 2. Schematic drawing of the mounting device used to assemble the various parts of the magnetometer.

vice, the torsion wire is glued to the Hysol posts with Stycast 2850 FT.[12] After curing *at room temperature*, the screws are removed, and the wheel is repositioned again along the wire if necessary. Finally, the platform of the wheel is also glued to the torsion wire with nonmagnetic Stycast 1266,[12] with about 30° horizontal inclination. After curing, the wire in the middle of the platform is not removed in order to avoid that the adhesion between the wire surface and the Stycast yields under the tension extended by the wire.

Stainless steel minicoaxial wires are attached to the electrodes with silver paint and are mechanically fixed to the housing with some epoxy glue. The coaxials and other wires (for thermometry and the feedback coil) run through holes in the bottom of the housing, so that they can eventually be fed through a conical plug or some other recipient to which the device is mechanically fixed.

IV. RESOLUTION AND OPERATION

We first discuss the resolution limits imposed by the detection technique and the mechanical properties of the device described in the previous sections.

The total value of the capacitance $C_{ac}+C_{bc}$ between the A and B electrodes and the C electrodes is found to be in the range of a few pF, in line with a simple estimate based on the total electrode surface area and the gap. The actual entity that is measured in an experiment is the ratio R_c

$$R_c=\frac{C_{ac}}{C_{ac}+C_{bc}} \tag{1}$$

which to first order is only sensitive to rotations and not to translations parallel or perpendicular to the rotation axis. This noise rejection technique complements the noise reduction by symmetry. The measurement of the capacitance ratio is done in a standard ac (1–10 kHz) bridge circuit using a ratio transformer.[1] The nulling of the bridge is performed with a lock-in amplifier.

The accuracy in the ratio measurement is typically about 1 ppm, which represents the electronic detection limit. The resolution is often somewhat worse due to mechanical vibrations, especially when using the smaller torsion wire diameters. Given this limit, one can estimate the smallest change in the torque that can be detected (the torque resolution of the device) in the ideal case as

$$\delta\Gamma=10^{-6}\,\frac{2\pi^2}{N}\,\frac{GR^4}{l}, \tag{2}$$

where N represents the number of C electrodes, G is the shear modulus of the wire, R the radius of the wire, and l its length outside the platform. In this equation we have taken into account that the two halves of the length l of the torsion wire act in parallel. For a 25-μm-diam phosphor bronze wire ($G=4\times10^{10}$ Nm^{-2}) of 1 cm length and with 8 C electrodes, the estimated sensitivity is around 0.2 pNm, consistent with the experimentally observed lowest torque resolution of a few times 0.1 pNm. At a magnetic field of 10 T this amounts to a magnetization resolution of a few times 10^{-14} J/T or, equivalently, a few times 10^{-11} emu.

Actually, the values for the resolution predicted by Eq. (2) form a lower limit. Due to parasitic capacitances in the wiring and to edge effects, the range over which R_c varies is less than 1, which can lead to a decrease in electronic sensitivity up to a factor of 5. The edge effects increase progressively as the number of electrodes is increased and the gap between the electrodes becomes comparable to their areal dimensions. The sensitivity of the detection of the rotation then increases no longer with the number of electrodes, which provides a practical limit for this number.

An important parameter is the response time of the system, which is determined by the resonant frequency of the device given by

$$f=\left(\frac{GR^4}{2\pi lI}\right)^{1/2}, \tag{3}$$

where I represents the moment of inertia of the rotor (and sample). It shows that the least amount of material used gives the highest eigen frequency, and therefore the shortest response time $\tau\approx1/2\pi f$. For the range of wire diameters given above and in the case of the solid state sample magnetometer, this frequency is higher than 1.5 Hz, depending slightly on the mass of the sample. This is high enough to take data with a 1 or 3 s time constant on the lock-in at a typical sweep rate of about 0.5 T/min.

We now discuss a few other features of the present design including linearity, feedback and forward bias capabilities, magnetic damping, and modularity. Contrary to those cases[2–5] where the gap between the electrodes is varied, the deviation from linearity between the torque and the capacitance change is small in our device, even for large excursions. As an example, for a magnetometer with eight electrodes we have found this deviation to be about 2% for a deflection of 10% full scale (full scale deflection corresponds thus to a 22.5° rotation). In case a better linearity is needed, the torque magnetometer can be operated in feedback mode with the coil mounted on the rotatable wheel. Feedback operation ensures a strictly linear relationship between the feedback current and the magnetization. Forward biasing (simpler than feedback) can be used when a sample having a large background magnetization is measured. Here, the background can be largely eliminated by passing a current through the coil which is a constant or proportional to the magnetic field or a combination of both. For de Haas-van Alphen measurements we have found this procedure to work

well. For example, it allows the field range of 1–20 T to be scanned in one single sweep without readjustment of the bridge at a sensitive lock-in setting (i.e., sensitive enough to observe the mechanical noise). A third purpose of the coil is to provide a torque calibration, which can be performed in the same run as the actual measurement.

The damping of the resonant motion of the wheel in a magnetic field is dominated by dissipation of eddy currents in the C electrodes. Without this mechanism, the damping of the resonant motion is far from critical and the damping time of the magnetometer can become many minutes in zero magnetic field. In fields of a few tesla this time is reduced to a few seconds and decreases further as B^{-2}. This is a valuable property since the field fluctuations and vibrations in a Bitter magnet increase considerably as the field is increased.

The modular design has the advantage that if, e.g., the torsion wire breaks, only the Hysol posts and the torque wire need to be replaced. Since the construction of the housing is quite time consuming this is an important property of the present design.

V. RESULTS AND DISCUSSION

The signals obtained with empty magnetometers always show a strong variation at low fields ($\leqslant 1$ T) of the order 1 nNm. These signals are independent of the field gradient, indicating that they stem from an anisotropic magnetization. In the magnetometers with Ag painted electrodes the variation of the background signal above 1 T is mainly due to an isotropic magnetization and can indeed be reduced to almost zero by positioning the device in the center of the field (see discussion further on). This small background signal is attributed to the slight off-axis position of the magnetic center of mass of the wheel. It stresses the importance of using the least amount of material possible.

For the magnetometer constructed with Au electrodes we have found a larger background variation which does not depend on the field gradient. Although the differences in background between magnetometers with Au and Ag electrodes are not well understood and still under investigation, we have been able to perform accurate magnetization measurements with both magnetometers and we now present some illustrative examples.

An example of the performance of the solid state sample magnetometer is given in Fig. 3, which shows the two-dimensional de Haas-van Alphen effect in the magnetization of a single layer 2DEG[8] which also displays the integer quantum Hall effect (not shown in Fig. 3). The 2DEG sample was a single AlGaAs-GaAs quantum well of about $4\times 4\ \mathrm{mm}^2$ on a 0.4 mm thickness GaAs substrate. It had a carrier density of $7.6\times 10^{15}\ \mathrm{m}^{-2}$ and contained 10^{11} electrons only (i.e., 1.6×10^{-13} mol). Due to this low electron density, there is a limited number of occupied Landau levels even at moderate magnetic field, and we plot the oscillating magnetization versus the number ν of filled Landau levels. We see a gradual transition from sawtoothlike oscillations to a more sinusoidal shape as ν increases. Note that the amplitude decrease is far from exponential, which is as expected for the 2D dHvA effect in contrast to the 3D case.

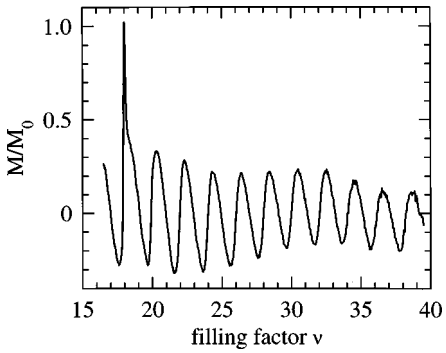

FIG. 3. The dHvA magnetization per electron of a two-dimensional electron gas at a temperature of 0.5 K showing sawtoothlike oscillations. The magnetization is normalized to the expected value for noninteracting electrons $M_0 = e\hbar/2m^*$, where m^* represents the effective electron mass. The measurements were performed in a Bitter magnet. At the high field side of the last oscillation one observes a nonequilibrium current peak.

A second contribution to the signal which is often observed,[6,13] stems from nonequilibrium currents in the 2DEG around integer ν, induced by the sweeping of the field when the sample is in a state of nearly zero resistance. This effect is visible in the high field flank of the last magnetization oscillation in Fig. 2.

The magnetization was measured in a Bitter magnet at a temperature of 0.5 K. The magnetometer was positioned slightly above the liquid ^{3}He level in the cryostat, and a Cu wire coil foil, extending into the liquid ^{3}He, surrounded the magnetometer. In this case the torsion wire was a ϕ 25 μm phosphor–bronze wire. The resolution of this measurement is about 1 pNm, while in a superconducting magnet the resolution is typically a factor of 2 to 3 better.

The tiny anisotropic magnetic moment **M** of the 2DEG is due to the orbital magnetism of the electrons (cyclotron orbits) and it is constrained to be perpendicular to the plane of the 2DEG, whose normal has been tilted about 30° with respect to the magnetic field **B**. The measured torque $\boldsymbol{\Gamma}$ is therefore equal to $\mathbf{M}\times\mathbf{B}$, and **M** is obtained by dividing the measured torque by $B \sin\theta$.

An advantage of the present design is that the sample is located far away from the electrodes and that spurious signal arising from coupling of the ac measuring electric field to the sample is negligible (unlike in the designs of Refs. 1, 2, and 6).

The second example we present is a measurement of the isotropic nuclear magnetization of liquid ^{3}He. As already described, here the magnetometer wheel was a solid cylinder with a small hole, in which the liquid ^{3}He is located at a horizontal distance $r = 4$ mm away from the rotation axis. The whole magnetometer was immersed in liquid ^{3}He contained in a pressure cell, avoiding the need to attach a filling capillary to the wheel itself. Because the moment of inertia of the wheel was much larger than in the previous example, a torsion wire of ϕ 100 μm was used.

Figure 4 shows the slow relaxation of the nuclear magnetization of liquid ^{3}He towards its final value after a fast step of the applied magnetic field, at a constant temperature of 80 mK. The two curves shown were obtained with the same magnetometer, respectively, in a Bitter magnet at the

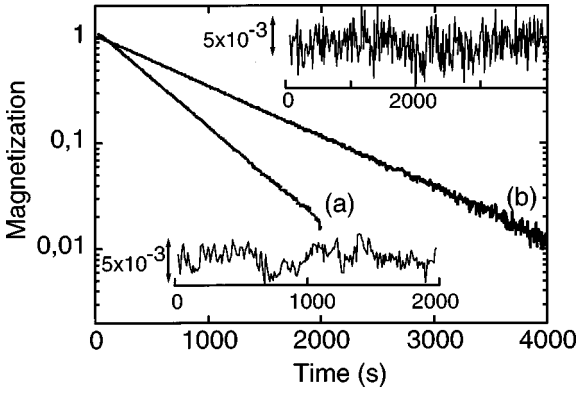

FIG. 4. The relaxation of the nuclear magnetization of liquid ^{3}He at a temperature of 80 mK following a fast field step: (a) in a hybrid magnet at a pressure of 25 bar, and (b) in a Bitter magnet at a pressure of 2 bar. At $t=0$ the magnetic field is halfway the fieldsweep [(a) from 21 to 23 T at about 0.5 T/s and (b) from 1 to 5 T at 0.33 T/s]. Magnetization scale has been normalized by the magnetization change expected from NMR (see the text). Typical values are shown on the right axis. Deviations from the best two exponential decays are shown in the insets, showing the typical stability over long time periods.

Grenoble HMFL (1–5 T sweep, at a pressure of 2 bar) and in the 25 T hybrid magnet at the Nijmegen HFML (21–23 T sweep, at a pressure of 24 bar). In both cases the wheel was located about 5 cm from the field center, so that the local field was typically 0.85 times its central value and the ratio $\nabla B/B \approx 5\ \mathrm{m}^{-1}$. The difference in the relaxation times is due to the combination of different pressures and final magnetic fields.[14] The measured torque was converted to an absolute magnetization as discussed in Sec. II, and the magnetization changes were normalized by the expected values inferred from the NMR measured susceptibility.[15] As can be seen from Fig. 4, the curve measured at low pressure does indeed extrapolate to close to the expected value of unity at zero time (which is taken as the half-sweep time, so as to properly account for the relaxation during the sweep duration). At 24 bar the signal is about 20% higher than expected. This effect, which was also observed at the Grenoble HMFL, is not yet understood, but has to be ascribed to some mechanical effect of pressure on the magnetometer.

Let us now comment on Fig. 4 in terms of sensitivity and noise. For both curves, the absolute value of the magnetization step is of the order of $2.5\times10^{-7}\ \mathrm{Am}^2$ (2.5×10^{-4} emu), corresponding to a nuclear polarization of 0.5% for the studied volume of 0.17 cc. The relaxation can be followed over two decades, evidencing a good long term stability (≈ 1 h). As shown by the inset of Fig. 4, the long term noise is indeed equivalent to about $\pm 0.2\%$ of the total step, or 10^{-6} emu. We stress that such a stability requires an excellent stability of the field gradient. As an example let us consider the 21–23 T step. Due to the large background susceptibility compared to the ^{3}He susceptibility (about 10 times larger in this case), combined with the ≈ 10 times ratio between the final field and the field step, a 1% resolution on the nuclear magnetization step requires a 10^{-4} stability of the field gradient, or of the distance from the wheel to the field center (which means a 5 μm stability). This shows the critical importance of reducing as much as possible the background signal.

In these experiments, the rms torque noise measured on a 100 s time scale was of the order of 50 pNm, independent of the magnetic field, corresponding to a magnetization noise varying as B^{-1} and of about 2×10^{-7} emu at 15 T (for $\nabla B/B = 5\ \mathrm{m}^{-1}$ and a distance between the hole axis and the torsion wire $r=4$ mm). This is much larger than for the solid sample case due to two reasons. First, the present device is heavier and more sensitive to vibrations, giving a higher torque noise. Second, the method is intrinsically less sensitive for a liquid sample than for a solid sample since $r\times M\nabla B$ is typically 50 times smaller than MB.

We finally note that this discussion of liquid ^{3}He also pertains to the case where a solid state magnetometer would be cooled below 0.3 K by insertion into the mixing chamber of a dilution refrigerator. One should then be aware of the magnetic buoyancy exerted by the mixture when the magnetometer is not perfectly symmetric. Similar to what is shown in Fig. 4, there will be an instantaneous diamagnetic contribution and a slowly relaxing paramagnetic part which looks like drift in the magnetometer signal.

ACKNOWLEDGMENTS

We thank A. Benoit and B. Castaing for useful suggestions in the early stages of this work and M. Specht and L. Lévy for their interest and for suggestions on the Au evaporation. We also thank T. Crozes and B. Pannetier for the inventive Au evaporation and M. Potemski and Zb. Wasilewski (NRC, Ottawa, Canada) for supplying the 2DEG sample. We are indebted to F. G. Derksen, L. Perli, and J. Spitznagel for expert technical support. This work is supported in part by 'De Stichting FOM', which in turn is financially supported by NWO, and by the European Community through the TMR programme under Contract No. ERBFMGECT950077.

[1] J. P. Eisenstein, Appl. Phys. Lett. **46**, 695 (1985).
[2] I. M. Templeton, J. Appl. Phys. **64**, 3570 (1988).
[3] J. S. Brooks, M. J. Naughton, Y. P. Ma, P. M. Chaikin, and R. V. Chamberlin, Rev. Sci. Instrum. **58**, 117 (1986).
[4] A. G. Swanson, Y. P. Ma, J. S. Brooks, R. M. Markiewicz, and N. Miura, Rev. Sci. Instrum. **61**, 848 (1990).
[5] M. Bravin, G. Remenyi, S. A. J. Wiegers, L. Puech, and P. E. Wolf, Physica B **194–196**, 745 (1994).
[6] S. A. J. Wiegers, J. C. Maan, and C. T. Foxon, Physica B **211**, 474 (1995).
[7] M. Chaparala *et al.*, AIP Conf. Proc. **273**, 407 (1993).
[8] S. A. J. Wiegers *et al.*, Phys. Rev. B **79**, 3238 (1997).
[9] A. S. van Steenbergen, S. A. J. Wiegers, M. Bravin, and P. E. Wolf, Physica B **211**, 316 (1995); A. S. van Steenbergen, S. A. J. Wiegers, J. A. A. J. Perenboom, and J. C. Maan, Czech. J. Phys. **46**, 239 (1996) Suppl. S1.
[10] U. Zeitler *et al.*, Physica B **211**, 381 (1995).
[11] Hysol Epoxy CP4-4285, The Dexter Corporation, Olean, New York, U.S.A. Hysol is a softer material than Araldite and has better machining properties.
[12] Stycast 1266 and Stycast 2850 FT, Emerson and Cumming.
[13] C. L. Jones *et al.*, Solid State Commun. **95**, 409 (1995).
[14] A. S. van Steenbergen, S. A. J. Wiegers, J. A. A. J. Perenboom, and J. C. Maan, Phys. Rev. Lett. **79**, 115 (1997).
[15] H. Ramm, P. Pedroni, J. R. Thomson, and H. Meyer, J. Low Temp. Phys. **2**, 539 (1970).